

Bactericidal Activity of Copper Oxide Nanocomposite/Bioglass for in Vitro Clindamycin Release in Implant Infections Due to *Staphylococcus aureus*

Zohre Alijanian,^{1,*} Nasrin Talebian,² and Monir Doudi¹

¹Department of Microbiology, Faculty of Biological Science, Falavarjan Branch, Islamic Azad University, Falavarjan, Isfahan, IR Iran

²Department of Chemistry, Faculty of Biological Science, Shahreza Branch, Islamic Azad University, Shahreza, Isfahan, IR Iran

*Corresponding author: Zohre Alijanian, Department of Microbiology, Faculty of Biological Science, Falavarjan Branch, Islamic Azad University, Falavarjan, Isfahan, IR Iran. Tel: +98-3137420136, E-mail: Alijanian.Z@gmail.com

Received 2016 April 28; Revised 2016 June 18; Accepted 2016 June 20.

Abstract

Background: In recent years, bioactive bioceramics such as bioglass and hydroxyapatite (HA) have been introduced as a remarkable development in the field of medicine due to their bio-adaptability, non-toxicity, and persistence, in vivo. They have many potential applications in the repair of bone defects and hence they have attracted significant interest from scholars.

Objectives: The aim of this study was to synthesize inorganic matrix CuO-based bioglasses and evaluate their antibacterial activity against aerobic bacterial infections in bone implants.

Methods: Nano-composite samples of silica-based bioactive glass, 60S BG with nano-powder CuO, were synthesized using the sol-gel method and then assessed with regard to their antibacterial properties against *Staphylococcus aureus* using well diffusion agar. The samples included BG58S (58%SiO₂, 36%CaO, 6%P₂O₅), BG/10CuO (58%SiO₂, 26%CaO, 6%P₂O₅, 10%CuO), and BG/20CuO (48%SiO₂, 26%CaO, 6%P₂O₅, 20%CuO). To evaluate their bioactivity, the prepared samples of BG/20CuO, BG/10CuO, and BG58S were immersed in simulated body fluids (SBF). The surface morphology and structure of the samples before and after immersion in the SBF were characterized using scanning electron microscopy (SEM) and Fourier transform infrared (FTIR), respectively. Then, the BG/20CuO and BG/10CuO samples were loaded in clindamycin, an antibiotic widely used in the treatment of osteomyelitis, and their release profiles were studied in phosphate buffer solution.

Results: It was observed that the growth inhibition zone increased through clindamycin release due to the increasing CuO percentage in the nanocomposite of bioactive glass. The bioactivity of the nanocomposite/bioglass with CuO was superior to that of bioglass alone. In this study, the BG/20CuO sample showed a sustained release of clindamycin, which is sufficient for a drug delivery system.

Conclusions: Increasing the Cu nanoparticles in bioactive glass samples leads to the release of Cu²⁺, which has a positive effect on the antibacterial mechanism, as well as decreasing the cultured *Staphylococcus* colonies found on the bioglasses. Therefore, it seems that the nanocomposite/bioglass of CuO is a promising option for aerobic bacterial inhibitor systems in common bone implant infections.

Keywords: Bioactive Glass 58S, Bone-Implant Interface, Clindamycin, Diffusion Antimicrobial Tests

1. Background

In recent years, the field of nanoscience and nanotechnology has achieved significant advances with nanosized inorganic and organic particles that are subject to increasing applications as amendments in industrial, medicine and therapeutics, synthetic textiles, and food packaging products (1). Furthermore, as biological phenomena develop at the nanoscale and because nanoparticles are highly biocompatible, they are increasing being used in the in vivo/in vitro medical research field, mainly in targeted drug delivery, imaging, sensing, and artificial im-

plants (2, 3). Their antimicrobial activity has been found to be a function of the surface area in contact with the microorganisms, and metal nanoparticles have many applications due to the antimicrobial activity when embedded and coated onto surfaces (4). Some nanocarriers designed for antibiotic delivery have proved to be essential due to their good potential for effectively managing pathogen-based diseases as an alternative and successful approach to the inhibition of antimicrobial resistance (5). Combination drug therapy boosts the immune system to eliminate hazardous micro-organisms, and the use of nano-based techniques is intended to change the properties of

microbial surfaces to overcome the developed antibiotic resistance when compared to single drug therapy (6).

Implants are predisposed to infection due to their supporting the growth of all kinds of micro-organisms, which has resulted in major objections to the extended use of implant devices and, ultimately, to the omission of this therapeutic option (7). These infections involve both the related tissues that face subsequent destruction and the blood (8). Thus, the implants require the long term enhancement of their host defenses and frequent persistence against bacterial colonies. The bacterial biofilm that develops on an implant's surface protects the organisms from both the host's immune system and antibiotic therapy (9). Biomaterial can be modified using antibacterial agents composited with implant surfaces through the loading capacity and drug release profile (10). *Enterococcus faecalis* involves the root canal system (11), although complicated infections developed with several pathogens such as *Staphylococcus aureus*, *Staphylococcus epidermidis*, *Escherichia coli*, and other micro-organisms from the *Proteus* genus result in bone inflammation and destruction as common surgical complications (12).

Over the last few years, research interest in bioactive bioceramics has increased in the medical community, especially with regard to the application of 45S5 and silicate-phosphate glasses in bone tissue engineering (13). Some remarkable properties of materials such as hydroxyapatite and bioactive glasses include osteogenesis behavior, the ability to be grafted into soft tissue as well as hard tissue, the formation of a layer of hydroxycarbonate apatite in biological fluids (14), stimulation of gene expression in bone-generating cells (15), antibacterial activities (16), and anti-inflammatory effects (17), all of which have been investigated for the purpose of bone tissue engineering (15, 18).

Additionally, their ability to deliver drugs as well as to stimulate effective ion diffusion in bodily fluids is applicable for osteogenesis, especially in order to suppress bacterial infection following surgery. Bioactive scaffolds along with osteoconductive factors (to guide the growth of new bone), induced osteogenesis (to promote new bone formation), and angiogenesis (to build blood vessels) are significant advantages for repairing serious bone defects (19, 20) when compared to conventional treatments such as systematic antibiotic therapy, necrotic tissue/foreign object removal after surgery, wound drainage, and implant removal (21), which all have limitations that might lead to additional surgical intervention for patients (21, 22).

Although a bioactive coating material such as HA can be sprayed onto the surface of dental metal implants, its flaws (23) are apparent even in instances of good adhesion and researchers have hence sought to find additives to improve this issue in titanium implants (24). For disinfection

purposes, bioactive glasses have shown no side effects in root canal therapy (19) due to several probable mechanisms, including the inhibition of bacterial colonization, a pH increase in aquatic solutions, and calcium levels (25-27). However, calcium hydroxide indicated a better antimicrobial effect than bioactive glass (28). To control common pathogenic microorganisms in implant sites, especially *Staphylococcus aureus* and *Staphylococcus epidermidis* (29), researchers have considered bioactive glass-based materials because of their good potential as carrier systems for drug-antibiotic release intended to inhibit bacterial growth in dental cysts both in vitro and in vivo (30).

In order to overcome the abovementioned defects, metal oxide nanoparticles were doped with bioceramic particles with many applications for medical disinfection, the food industry, and other industries (31-33). Silicate-based bioactive glasses doped with copper oxide have also been studied due to the importance of copper in osteogenesis (34) and the stimulation of the growth factor FGF-2 in vitro (35).

Generally, two basic procedures exist for the determination of nanoparticle sizes, and they can be performed with the suspension of dry powders by numerous commercially available instruments. The first method involves inspecting the particles and taking actual measurements of their dimensions. Microscopic techniques, for example, can measure many dimensional parameters from particle images. The second method utilizes the equivalent spherical size in the linear relationship between a particle's behavior and its size. For example, in photon correlation spectroscopy (PCS) the dynamic fluctuation of the scattered light intensity is the basis for the calculation of the average particle size. Therefore, the information is not reported as exact sizes, but rather as the average particle size and the distribution of sizes about that average (36). In this study, for instance, the average particle size of the prepared nanoparticles was analyzed using X-ray diffraction spectroscopy.

2. Objectives

The main purpose of this study is the antibacterial evaluation of silicate-based bioglasses doped with CuO as a mineral matrix and immersed in simulated body fluid (SBF). This metal oxide bioglass nanocomposite is designed for the controlled antibiotic release of clindamycin against one of the most common infectious pathogens in implants, namely *Staphylococcus aureus*.

3. Methods

3.1. Materials

The chemicals required for the preparation of the SnO₂ sol solution and the SBF solution were used according to the recommendations of Bohner and Lemaitre (37).

3.2. Preparation of the BG Powders

The glasses were synthesized using the sol-gel process with the following compositions:

1) For the undoped bioactive glass known as B58S: 58%SiO₂, 36%CaO, 6%P₂O₅.

2) For the Cu-doped bioactive glasses with a different percentage of metal oxide known as BG/10CuO: 58%SiO₂, 26%CaO, 6%P₂O₅, 10%CuO, and BG/20CuO: 48%SiO₂, 26%CaO, 6%P₂O₅, 20%CuO.

First, the hydrolysis of tetraethyl orthosilicate (BG: 10.04 mL, BG/10CuO: 23.5 mL, BG/20CuO: 19.23 mL) was catalyzed with 30 mL of a 0.1 M solution of HNO₃ and then stirred for 30 minutes. The sols were obtained after adding the other reagents, including triethyl phosphate (BG: 1.52 mL, cu-doped BGs: 3.80 mL), calcium nitrate tetrahydrate (BG: 12.27 g, cu-doped BGs: 30.69 g), and copper (II) acetate monohydrate for the BG/10CuO and BG/20CuO (0.7 and 1.7 g, respectively), sequentially in order to compose the desired gels with 45 intervals under constant stirring.

When the final reagent was added, the obtained sols were allowed to complete hydrolysis for 1 hour at room temperature. The resultant sols were poured into capped PTFE vessels and then stored for 10 days at room temperature in order to transform from homogenous sol to gel. After the ultrasonic procedure was performed on the obtained gels for 30 min, they were oven-dried at 60°C for 20 hours. The dried gels were subject to further heat treatment in an oven as follows: 90°C (24 hours), 130°C (40 hours), 100°C (2 hours), 300°C (1 hour), and 700°C (5 hours). Finally, the BG powder samples were prepared by crushing the dried gels.

3.3. Methods of Characterization

3.3.1. Chemo-Physical Properties

To identify the structural characterization and surface morphology of the non-doped BG58S and Cu-doped BG20CuO, the required analysis was performed using various pieces of equipment. An elemental analysis was performed to determine and confirm the accurate molar ratio of the elements and oxides in the synthesized samples. Fourier transform infrared (Spectrum 65 FTIR spectrometer, PerkinElmer Inc., Waltham, MA, USA), scanning electron microscopy (SEM, Philips XL 30, SEMTech Solutions, Inc., North Billerica, MA, USA), and X-ray diffraction spectroscopy (XRD, Bruker D8 advance, Bruker Co., Billerica,

MA, USA) techniques were used to characterize the prepared bioactive glass samples. The SEM graphs and XRD patterns were assessed to investigate the surface morphology and particle size, while the FTIR spectra were used to monitor the types of bonds present in the glass network.

3.3.2. Antibacterial Tests

To prepare the bacterial culture, *Staphylococcus aureus* (*S. aureus*, PTCC 1431) was purchased from the Persian type culture collection and nutrient broth (NB) was used as a growing medium for both the microorganisms at 37°C for 20 hours. First, a culture of the bacteria was prepared on nutrient agar medium (NA) and then, with a sterile loop, 4-5 colon bacteria were removed and added to 5 mL distilled water to prepare the microbial substance. It must be noted that the amount of cultured bacteria added to the distilled water was sufficient that its turbidity would be equivalent to 5.0 McFarland (1.5×10^8) standards. We used the minimal inhibitory concentrations (MIC) method to test the antimicrobial activity. The MIC is the lowest concentration of an antimicrobial material that will inhibit the visible growth of a microorganism after incubation. Different concentrations ($\mu\text{g}/\text{mL}$) of the composited nanostructures were used in the present study to determine the MIC.

To determine the potential antibacterial inhibitory effect of the BG materials on *S. aureus*, the bioactive glass powder samples were seeded on well plates at 0.02, 0.04, and 0.06 gr per well in a culture media inoculated with *S. aureus* and left to grow according to the McFarland standard for 24-48 hours until an inhibitory zone was formed. For the negative and positive controls, some wells were treated with physiological serum and an antibiotic, respectively. All the samples were assayed in tetraplicate and, for each experiment, the zone diameters of bacterial growth inhibition by the bioactive glass powders were measured, which indicates the antibacterial effect of the corresponding BG sample. Then, the minimal inhibitory concentration was calculated and the best samples were selected for a bioactivity assay.

3.3.3. In Vitro Bioactivity Assay

In order to monitor the hydroxyapatite coatings formed on the surface of the selected BG powder samples, the prepared monolith samples (0.06 g) were immersed in a simulated body fluid at a 37°C temperature for 1, 7, 14, and 28 days. Then, the samples were removed from the solution. The variation of the pH in the SBF was continuously recorded using a pH meter over a four-week period. The formed hydroxyapatite coatings were assessed to determine the crystalline phase, functional groups, and surface morphology of the monolith BG samples using a UV-vis spectrophotometric assay (MPC-2200, Shimadzu

Co., Tokyo, Japan) before and after their immersion in the SBF.

3.4. Clindamycin Loading Process

For the preparation of the PBS solution, a protocol was used as described by Kokubo (14). For the clindamycin loading process, we immersed the BG58S and BG/20CuO (selected as the best samples according to the antibacterial assay) in clindamycin (7 mg/mL) enriched PBS (KH_2PO_4 : 0.05 mol/L, NaOH: 0.04 mol/L) autoclaved at 37°C for 6 hours. Then, the samples were removed from the PBS and rinsed thoroughly in fresh PBS three times to remove the unloaded antibiotic.

To assess the in vitro release from the bioactive glasses, a UV-vis spectrophotometer was used to evaluate the amount of released clindamycin, and the obtained spectra were compared before and after immersion in the PBS. The calibration curve was used to calculate the loaded clindamycin based on the antibiotic concentration from the following relationship:

$$\text{Antibiotic loading (\%)} = \frac{[(\text{Volume of antibiotic solution, mL}) \times (\text{Antibiotic concentration after loading} - \text{Antibiotic concentration before loading as 7mg/mL})] / (\text{Weight of the scaffold, g}) \times 100.}$$

The scaffolds coated with clindamycin were maintained in the drug solution at 4°C prior to starting the drug release test in order to prevent their degradation by light and temperature.

3.5. The Release Profile of Clindamycin

To assess the clindamycin released from the antibiotic-loaded BG samples, 35 mg of the loaded samples was immersed in 10 mL of PBS and kept for 2, 6, 12, and 48 hours. After each time interval, 2 ml of PBS was collected and replaced with 2 ml of fresh PBS. The collected PBS was assayed at a max $\lambda=297$ nm using the UV-vis spectrometric method. The calibrated curve for the antibiotic loading process was prepared based on different antibiotic concentrations. The release profile of clindamycin from the loaded bioactive glasses was determined using the plotted curve.

4. Results

4.1. Microstructural Characterization

4.1.1. FTIR Analysis

To identify the crystalline phase of the non-doped BG58S and Cu-doped BG20CuO before and after annealing, the FTIR spectroscopy results were interpreted to determine the functional groups for the various types of chemical bonding on the surface. A graph of the FTIR spectra of these bioactive glass samples in the range of 400-4000

cm^{-1} is presented in Figure 1. The FTIR results obtained from the synthesized samples indicated that the FTIR spectra in all the samples showed the basic absorption frequency bands in the ranges 450 - 550, 600 - 620, and 1100 - 1200 cm^{-1} to be related to the bending mode of Si-O-Si, the vibration mode of symmetric Si-O-Si stretch, and the vibration mode of asymmetric Si-O-Si stretch, respectively (38).

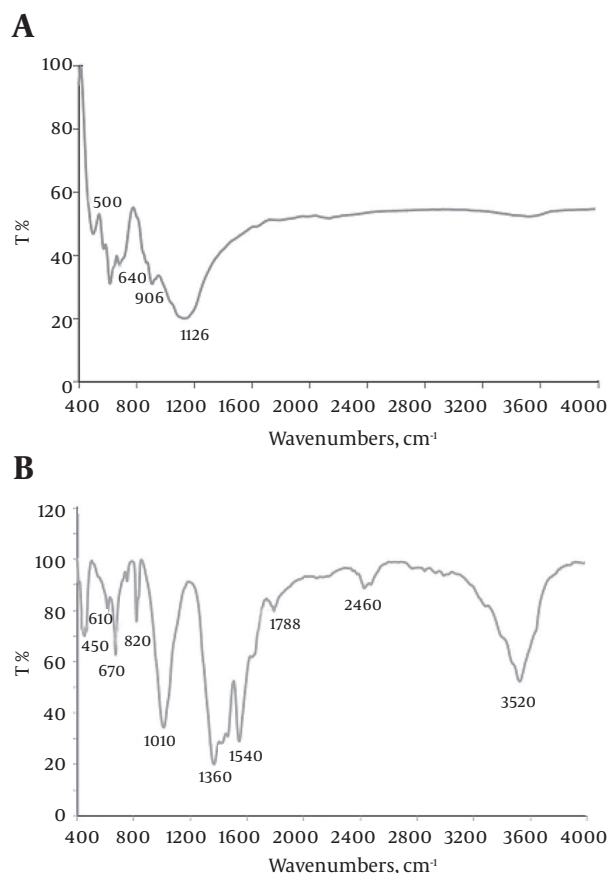


Figure 1. FTIR spectra of the bioactive glass samples; A, the non-doped BG58S and B, the doped BG/20CuO.

4.1.2. SEM Analysis

Figure 2 shows the scanning electron microscopy (SEM) images of the BG58S and BG/20CuO powder samples before and after annealing. In the case of BG58S, the large grain dimension of the bioglass crystallinity was observed according to the XRD results (data not shown), indicating very clearly the formation of crystal phases. The radius of the involved ions in the synthesized samples included: $r(\text{Cu}^{2+})$: 73 pm, $r(\text{Ca}^{2+})$: 94 pm, and $r(\text{Si}^{4+})$: 41 pm.

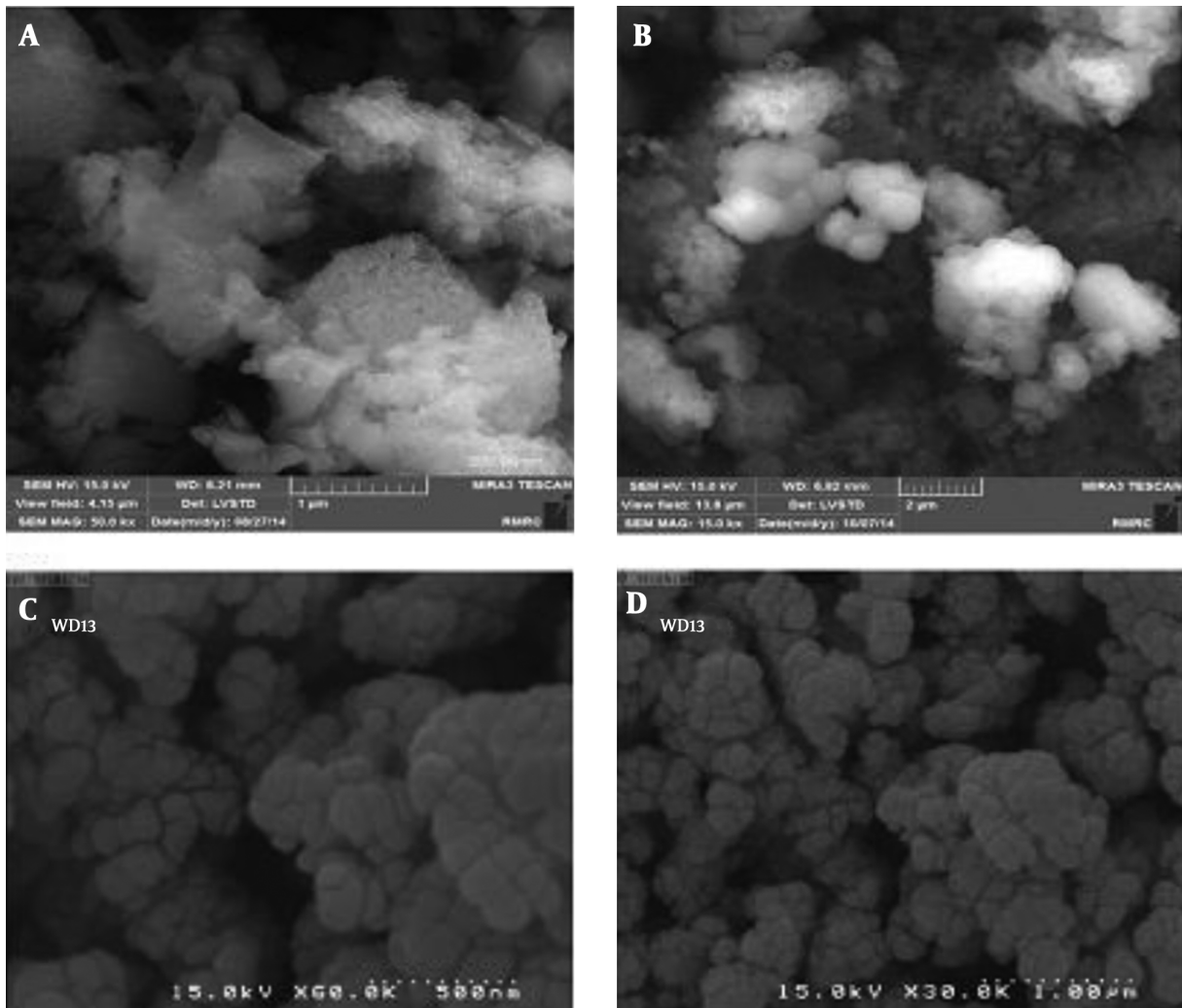


Figure 2. SEM micrographs of the bioactive glass samples, A) the non-doped BG58S and B) the doped BG/20CuO, at two different magnifications (sizes noted on each image).

4.1.3. XRD Patterns

The identified XRD pattern (data not presented here) showed a particle size of around 30-70 nm for the BG/20CuO powder samples.

4.2. Antibacterial Activity

Figure 3 reports the results concerning the bacterial inactivation properties of the studied powder samples against *S. aureus* according to the well plate-based method.

It can be observed from Figure 3 that the antibacterial effect of the bioactive glasses varies according to the bacterial species, chemical compounds of the bioglasses, and sample concentrations. The bioactive glass samples doped with CuO had an inhibitory effect on the growth of

S. aureus; therefore, it can be considered to be an antibacterial treatment. The observed inhibition zone of bacterial growth increased in diameter when the percentage of copper oxide and the amount of powder sample added increased. As the results of the antibacterial assays showed, the order of the bacterial inhibitory effect that the composed bioactive glasses showed against the growth of *S. aureus* is as follows: BG/20CuO > BG/10CuO > BG/58S.

4.3. In Vitro Bioactivity in SBF

4.3.1. Immersion in SBF with Clindamycin

To determine the clindamycin levels in the SBF in order to evaluate the antibiotic loading process in the best bioactive glass samples (i.e., BG/20CuO), a UV-vis spectrophotometric assay compared the spectra of samples in the initial

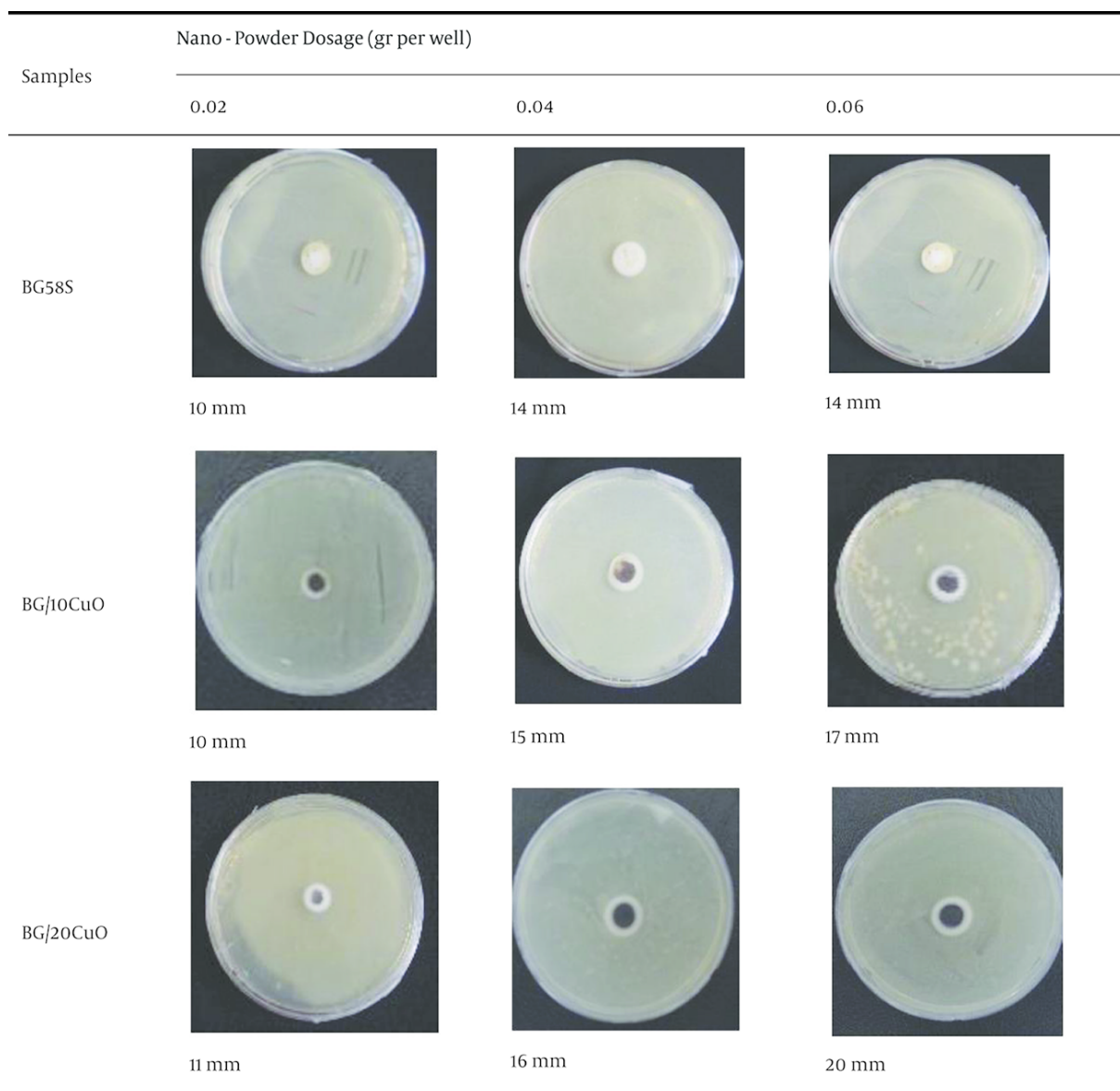


Figure 3. The zone of bacterial growth inhibition (in mm) on the *Staphylococcus aureus* culture obtained after adding Cu-doped bioactive glass nanocomposites (in gr per well). (Note: The nanocomposite samples showed antibacterial properties and inhibited the growth of *S. aureus* as a gram-positive bacterial model like the non-composite sample. BG58S: BioGlass58%SiO₂, BG/10CuO: BioGlass10%CuO, BG/20CuO: BioGlass20%CuO.)

PBS with those in the recovered PBS after immersion for 6 and 16 hours (Figure 4). A decrease in the antibiotic concentration compared to that in the initial PBS showed that the loading process of clindamycin on the surface of the bioactive glasses was actually performed.

4.3.2. The Released Clindamycin in SBF

The purpose of our study was to produce composite samples of silicate bioactive glasses doped with CuO in

order to evaluate their potential as a carrier for the controlled release of the clindamycin antibiotic in the *S. aureus*-induced infection common in bone cysts. Therefore, the release profile of the antibiotic from BG/20CuO in PBS was studied using a UV-vis spectrophotometric assay (Figure 5).

As shown in Figure 5, an initial release with an incremental slope of the curves was followed by a 19% - 24% release of clindamycin through 72 hours. This finding can be

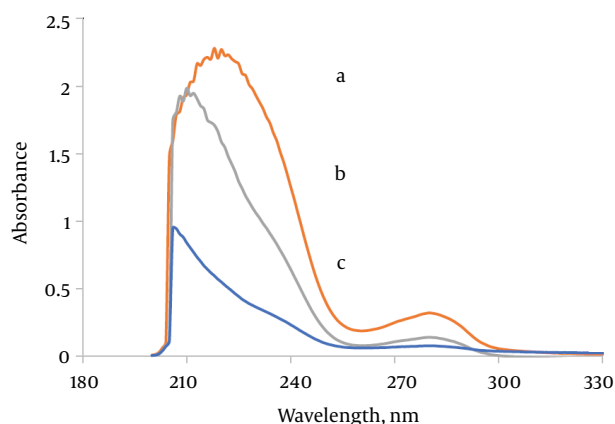


Figure 4. UV-vis spectra of BG/20CuO immersed in SBF with clindamycin a) before the release of the antibiotic, b) after the release of the antibiotic for 6 hours of immersion, and c) for 16 hours of immersion.

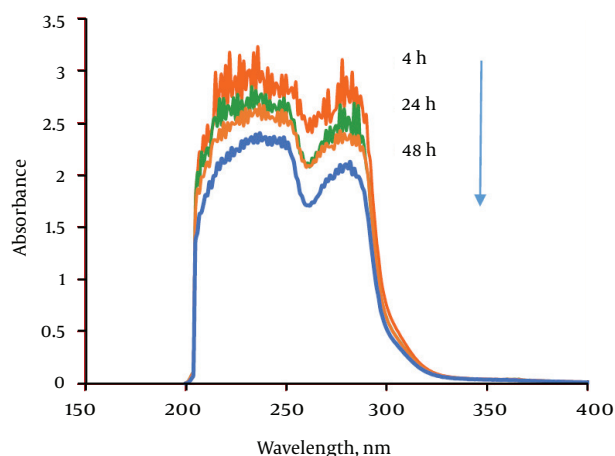


Figure 5. The Profile of the Released Clindamycin from BG/20CuO After Immersion in SBF for 4, 24, And 48 Hours

interpreted as the ability of our composed BG samples to act as a desirable and controlled system of drug release in a continuous and slow way.

5. Discussion

Bioactive glasses have been shown to have unique characteristics despite the fact that they can easily be broken or fractured. These characteristics include a speed-controlled ability to perform a break down process with free ion release and convert into an HA-like material that could be rigidly held in a strong bond with soft and hard tissues. In order to promote their bioactivity into a special biological response in the considered physiological conditions, sev-

eral approaches have been developed, including integrating bio-glasses with different metal ions and natural or synthetic organic polymers in a silicate network. The aim of the procedure is to promote the impact of bioglass stimulation on osteogenesis, angiogenesis, and antibacterial processes.

In 1971, Hench and colleagues studied bioactive glasses for the first time and developed them (39). Next, metal and non-metal oxides such as TiO_2 (40), ZnO (41), B_2O_3 (42), and other materials were applied to develop nanocomposites integrated with phosphate bioglasses for the regulation of solubility, stability of the glass network, and control of the destruction levels. As in the present study, other investigations focused on the modification of bioactive glasses and found various results. Feng et al. (1998) showed that biofilms of hydroxyl apatite saturated with silver resulted in remarkable antibacterial properties against positive and negative bacteria (43). Additionally, Chen et al. (2006) found that the application of hydroxyl apatite including silver showed a similar intensity of cellular toxicity in vivo when compared to in vitro for *Staphylococcus epidermis* and *Staphylococcus aureus* with highly decreased numbers (44).

In addition, Devadathan and Raveendran (2014) worked on polyindole-based nickel-zinc oxide nanocomposites to identify the antifungal properties, and they proved that a non-composite could be used as an antifungal material for the fungi *Penicillium Chrysogenum* (45). However, the use of animal models, as well as various treatment methods and nanoparticles with different concentrations and shapes, presents new horizons for further research to investigate the applications of nanotechnology (46). Some studies have emphasized the toxicity of nanoparticles in in vivo conditions, considering the molecular effects of some nanoparticles with different concentrations and shapes in the tissues of laboratory animals prior to use on humans (47). Significant scientific achievements involving nanotechnology have also been found for gold nanoparticles (48).

In this study, the fabrication and characterization of bioactive glasses containing nanocomposites with different CuO contents were found to inhibit implant-associated infections through clindamycin release. According to previous studies, certain ions play a role as nucleating agents in bioactive glasses (49). Therefore, it seems that the number of fabricated nuclei increases preferably instead of an increase in their sizes, resulting in a decrease in grain size in the presence of CuO and ZnO. Our SEM figures demonstrated this finding in bioactive glass samples doped with CuO. The remarkable decrease in grain sizes observed in the studied doped samples can influence the bioactivity, speed of solubility, and release of effective ions for osteo-

genesis in samples following SBF immersion in vitro.

Silicate bioactive glasses are treated at high temperatures and show different phases during annealing due to both the duration and temperature variations. For the sake of brevity, it is noted that the annealing temperature and its duration were the same for all the samples, and the weak diffraction in the modified samples is a clue to the crystal inhibition due to CuO.

The findings of the SEM analysis showed that a small difference between the ion modified crystal network (Ca^{2+}) and the Cu^{2+} ion led to the possibility of exchanging these ions with each other in both the bioglass composite and crystal network. The modifying ions in the network, including Na^+ , K^+ , and Ca^{2+} , influence the morphology of the surface and the grain dimensions (50). The SEM images of the nanocomposite samples with Cu^{2+} indicated a remarkable decrease in grain dimension. This influences bioactivity, the dissolution rate, and effective ion release in osteogenesis during the submersion of the samples in SBF in vitro. It was found that some ions cause nucleation in bioactive glasses (49). Therefore, it seems that in the presence of CuO, the number of nuclei formed is determined by their growth, which results in a decrease in particle dimensions.

The FTIR spectra of all the modified bioactive glasses in the presence of the metal oxide (CuO) indicate a slight variation in the situation of the bands and their intensity in comparison with BG58S. The bands that appeared at $1350 - 1450 \text{ cm}^{-1}$ and $2450 - 2460 \text{ cm}^{-1}$ for the bioactive glass samples are attributed to $(\text{CO}_3)^{2-}$ (the vibration mode of the symmetric and asymmetric C-O stretch, respectively), probably due to carbonating Ca^{2+} . The new bands at $2850 - 2950 \text{ cm}^{-1}$ for the modified bioactive glass samples are attributed to the vibration mode of the C-H stretch due to the broken bonds of carbonate in the bioactive glass network. The appearance of new bonds related to Si-O-NBO and their increased intensity at $820 - 830 \text{ cm}^{-1}$ and $1000 - 1100 \text{ cm}^{-1}$ in the modified samples in the presence of metal oxide indicate their function in the modification of the glass network. By studying the FTIR results, we found that CuO apparently functions as a constituent of the network and as a modifier of crystallinity for the bioactive glass samples.

Although there are no reports concerning the antibacterial activities of Cu-doped bioactive glasses, many different systems have been designed and studied with the aim of promoting antibacterial properties with the participation of Cu^{2+} or different forms of that element as thin films and powders. In the present work, the integration of Cu^{2+} in the bioactive glass samples brought about an improvement in the antibacterial effects. Additionally, other studies have shown an improvement in the antibacterial activities of bioactive glasses that are doped with elements such

as Zn^{2+} and Ag^+ in a silicate network.

In our samples, increasing the metal oxide percentage in the chemical structure of the bioactive glasses and increasing the amount of the powder samples caused an increase to be observed in the measured zone diameters of bacterial growth inhibition by the applied clindamycin antibiotic. An explanation for this finding is that the agar water is immediately absorbed into the applied antimicrobial material in the well and hence makes it diffuse into the agar medium. The antimicrobial material does not move through the agar medium with the same speed as the initial diffusion from the well into the agar medium. As a result, the concentration of the antimicrobial agent is highest around the well, and it reduces in a logarithmic fashion proportionally with the distance from the well. The speed of penetration via the agar medium is dependent on variables such as permeability, solubility, and the amount of antimicrobial material. Therefore, we can expect that the increased percentage of metal oxide in the chemical structure of the bioactive glass, as well as increasing the amount of the powder samples, makes the inhibition zone of bacterial growth increase in diameter.

The suggested mechanisms for the nanoparticles of CuO have been presented in several works, although the mechanism of photocatalytic bacterial inactivation has not yet been elucidated. It is suggested that the damage to the cell membrane occurs with the loss of K^+ ions, protein, and RNA from the bacterial cell, or else it is caused by an increase in Ca^{2+} ions due to the higher permeability of the cell membrane to these ions (51). In addition, it has been determined that the yield of antibacterial activity is defined according to a complex function with variables including the grain size and morphology, electron structure of the catalytic sample, speed of solubility, and nature of the microorganism considered for inactivation, in vitro. For example, an increase in Cu^{2+} of 1-10 mol% in a phosphate-based bioglass sample led to a decrease in solubility but, due to the higher proportion of special surface to volume, the release of Cu^{2+} ions indicated a positive effect on antibacterial activity and a decrease in the number of *Staphylococcus epidermis* cultured on a medium containing the composited bioglass sample (52). Further, the cell wall contains a very thick layer of peptidoglycan in these gram-positive bacteria, and the carotenoid pigments provide an integrative system for the membrane to be led into an improved resistance against oxidative stress. Damage to the bacterial cell is accelerated by the destructive superoxide anions produced through the internal bonding of CuO nanoparticles with the bacterial cell structure. Generally, the antibacterial properties of the composed bioglass samples were shown to be as follows: BG/20CuO > BG/10CuO. Apparently, the antibacterial synergetic effect

generated by the integration of two systems including CuO and bioactive glass leads to a higher yield of bacterial inactivation in our nanocomposite samples.

Finally, the findings we obtained from the development and evaluation of bioactive nanocomposites with CuO-doped glass designed for clindamycin release in order to inhibit implant infections showed that promoting the desirable bacterial inhibitory properties via antibiotic release in the designed nanocomposites can play an effective role in designing infection control systems in implants, especially those induced by *Staphylococcus* bacteria. In addition, these results provide further evidence of the more effective and higher bioactivity of our designed metal oxide nanocomposites when compared to the non-doped samples. The most important aspects for the application of these nanocomposites include higher bioactivity and, in turn, the faster improvement of hard tissues. It is suggested that the evaluation of the designed systems introduced in the present work should be repeated on cell cultures in vitro, preferably using the MTT test, and then on experimental animals in vivo. Additionally, attempts should be made to eliminate the drawbacks of bioactive glasses such as fracture in order to achieve more profitable and durable types. In the future, the effect of bioactive glasses should be studied in angiogenesis and chondrogenesis along with their application in bone tissue engineering.

Footnotes

Authors' Contribution: Study implication and design, data analysis and discussion, and all steps in preparing the manuscript: Zohre Alijanian, Nasrin Talebian, and Monir Doudi; microbiological technical and material support: Zohre Alijanian and Monir Doudi; nano-technological support and composite design: Nasrin Talebian; administration, acquisition of data, statistical analysis, and obtaining results: Zohre Alijanian, Nasrin Talebian, and Monir Doudi; study supervision: Zohre Alijanian.

Funding/Support: This research work was supported by a master's thesis grant from Islamic Azad university, Falavarjan branch.

References

- Gajjar P, Pettee B, Britt DW, Huang W, Johnson WP, Anderson AJ. Antimicrobial activities of commercial nanoparticles against an environmental soil microbe, *Pseudomonas putida* KT2440. *J Biol Eng*. 2009;**3**:9. doi: [10.1186/1754-1611-3-9](https://doi.org/10.1186/1754-1611-3-9). [PubMed: [19558688](https://pubmed.ncbi.nlm.nih.gov/19558688/)].
- Parak W. Biological applications of colloidal nanocrystals. *Nanotechnology*. 2003;**14**:15-27.
- Samia AC, Dayal S, Burda C. Quantum dot-based energy transfer: perspectives and potential for applications in photodynamic therapy. *Photochem Photobiol*. 2006;**82**(3):617-25. doi: [10.1562/2005-05-11-IR-525](https://doi.org/10.1562/2005-05-11-IR-525). [PubMed: [16475871](https://pubmed.ncbi.nlm.nih.gov/16475871/)].
- Martinez-Gutierrez F, Olive PL, Banuelos A, Orrantia E, Nino N, Sanchez EM, et al. Synthesis, characterization, and evaluation of antimicrobial and cytotoxic effect of silver and titanium nanoparticles. *Nanomedicine*. 2010;**6**(5):681-8. doi: [10.1016/j.nano.2010.02.001](https://doi.org/10.1016/j.nano.2010.02.001). [PubMed: [20215045](https://pubmed.ncbi.nlm.nih.gov/20215045/)].
- Allaker RP, Ren G. Potential impact of nanotechnology on the control of infectious diseases. *Trans R Soc Trop Med Hyg*. 2008;**102**(1):1-2. doi: [10.1016/j.trstmh.2007.07.003](https://doi.org/10.1016/j.trstmh.2007.07.003). [PubMed: [17706258](https://pubmed.ncbi.nlm.nih.gov/17706258/)].
- Krasner SW, Weinberg HS, Richardson SD, Pastor SJ, Chinn R, Sclementi MJ, et al. Occurrence of a new generation of disinfection byproducts. *Environ Sci Technol*. 2006;**40**(23):7175-85. [PubMed: [17180964](https://pubmed.ncbi.nlm.nih.gov/17180964/)].
- Zhao L, Chu PK, Zhang Y, Wu Z. Antibacterial coatings on titanium implants. *J Biomed Mater Res B Appl Biomater*. 2009;**91**(1):470-80. doi: [10.1002/jbm.b.31463](https://doi.org/10.1002/jbm.b.31463). [PubMed: [19637369](https://pubmed.ncbi.nlm.nih.gov/19637369/)].
- Hardes J, Ahrens H, Gebert C, Streitberger A, Buerger H, Eren M, et al. Lack of toxicological side-effects in silver-coated megaprotheses in humans. *Biomaterials*. 2007;**28**(18):2869-75. doi: [10.1016/j.biomaterials.2007.02.033](https://doi.org/10.1016/j.biomaterials.2007.02.033). [PubMed: [17368533](https://pubmed.ncbi.nlm.nih.gov/17368533/)].
- Monteiro DR, Gorup LF, Takamiya AS, Ruvollo-Filho AC, de Camargo ER, Barbosa DB. The growing importance of materials that prevent microbial adhesion: antimicrobial effect of medical devices containing silver. *Int J Antimicrob Agents*. 2009;**34**(2):103-10. doi: [10.1016/j.ijantimicag.2009.01.017](https://doi.org/10.1016/j.ijantimicag.2009.01.017). [PubMed: [19339161](https://pubmed.ncbi.nlm.nih.gov/19339161/)].
- Webster TJ, Ejirofor JU. Increased osteoblast adhesion on nanophase metals: Ti, Ti6Al4V, and CoCrMo. *Biomaterials*. 2004;**25**(19):4731-9. doi: [10.1016/j.biomaterials.2003.12.002](https://doi.org/10.1016/j.biomaterials.2003.12.002). [PubMed: [15120519](https://pubmed.ncbi.nlm.nih.gov/15120519/)].
- Waltimo T, Brunner TJ, Vollenweider M, Stark WJ, Zehnder M. Antimicrobial effect of nanometric bioactive glass 45S5. *J Dent Res*. 2007;**86**(8):754-7. [PubMed: [17652205](https://pubmed.ncbi.nlm.nih.gov/17652205/)].
- Vitale-Brovarone C, Miola M, Balagna C, Verne E. 3d-glass-ceramic scaffolds with antibacterial properties for bone grafting. *Chemical Eng J*. 2008;**137**(1):129-36. doi: [10.1016/j.cej.2007.07.083](https://doi.org/10.1016/j.cej.2007.07.083).
- Rezwan K, Chen QZ, Blaker JJ, Boccaccini AR. Biodegradable and bioactive porous polymer/inorganic composite scaffolds for bone tissue engineering. *Biomaterials*. 2006;**27**(18):3413-31. doi: [10.1016/j.biomaterials.2006.01.039](https://doi.org/10.1016/j.biomaterials.2006.01.039). [PubMed: [16504284](https://pubmed.ncbi.nlm.nih.gov/16504284/)].
- Kokubo T. Apatite formation on surfaces of ceramics, metals and polymers in body environment. *Acta Materialia*. 1998;**46**(7):2519-27. doi: [10.1016/s1359-6454\(98\)80036-0](https://doi.org/10.1016/s1359-6454(98)80036-0).
- Xynos ID, Edgar AJ, Buttery LD, Hench LL, Polak JM. Gene-expression profiling of human osteoblasts following treatment with the ionic products of Bioglass 45S5 dissolution. *J Biomed Mater Res*. 2001;**55**(2):151-7. [PubMed: [11255166](https://pubmed.ncbi.nlm.nih.gov/11255166/)].
- Allan I, Newman H, Wilson M. Antibacterial activity of particulate bioglass against supra- and subgingival bacteria. *Biomaterials*. 2001;**22**(12):1683-7. [PubMed: [11374470](https://pubmed.ncbi.nlm.nih.gov/11374470/)].
- Zhang D, Lepparanta O, Munukka E, Ylanen H, Viljanen MK, Eerola E, et al. Antibacterial effects and dissolution behavior of six bioactive glasses. *J Biomed Mater Res A*. 2010;**93**(2):475-83. doi: [10.1002/jbm.a.32564](https://doi.org/10.1002/jbm.a.32564). [PubMed: [19582832](https://pubmed.ncbi.nlm.nih.gov/19582832/)].
- Hench LL, Polak JM. Third-generation biomedical materials. *Science*. 2002;**295**(5557):1014-7. doi: [10.1126/science.1067404](https://doi.org/10.1126/science.1067404). [PubMed: [11834817](https://pubmed.ncbi.nlm.nih.gov/11834817/)].
- Hench LL, Thompson I. Twenty-first century challenges for biomaterials. *J R Soc Interface*. 2010;**7 Suppl 4**:S379-91. doi: [10.1098/rsif.2010.0151.focus](https://doi.org/10.1098/rsif.2010.0151.focus). [PubMed: [20484227](https://pubmed.ncbi.nlm.nih.gov/20484227/)].
- Kim TG, Shin H, Lim DW. Biomimetic scaffolds for tissue engineering. *Adv Funct Mater*. 2012;**22**(12):2446-68. doi: [10.1002/adfm.201103083](https://doi.org/10.1002/adfm.201103083).
- Zhao L, Yan X, Zhou X, Zhou L, Wang H, Tang J, et al. Mesoporous bioactive glasses for controlled drug release. *Microporous Mesoporous Mater*. 2008;**109**(1-3):210-5. doi: [10.1016/j.micromeso.2007.04.041](https://doi.org/10.1016/j.micromeso.2007.04.041).
- Wu C, Zhou Y, Xu M, Han P, Chen L, Chang J, et al. Copper-containing mesoporous bioactive glass scaffolds with multi-functional properties of angiogenesis capacity, osteostimulation

- and antibacterial activity. *Biomaterials*. 2013;**34**(2):422-33. doi: [10.1016/j.biomaterials.2012.09.066](https://doi.org/10.1016/j.biomaterials.2012.09.066). [PubMed: [23083929](https://pubmed.ncbi.nlm.nih.gov/23083929/)].
23. Allan I, Newman H, Wilson M. Particulate Bioglass reduces the viability of bacterial biofilms formed on its surface in an in vitro model. *Clin Oral Implants Res*. 2002;**13**(1):53-8. [PubMed: [12005145](https://pubmed.ncbi.nlm.nih.gov/12005145/)].
 24. Zehnder M, Waltimo T, Sener B, Soderling E. Dentin enhances the effectiveness of bioactive glass S53P4 against a strain of *Enterococcus faecalis*. *Oral Surg Oral Med Oral Pathol Oral Radiol Endod*. 2006;**101**(4):530-5. doi: [10.1016/j.tripleo.2005.03.014](https://doi.org/10.1016/j.tripleo.2005.03.014). [PubMed: [16545719](https://pubmed.ncbi.nlm.nih.gov/16545719/)].
 25. Wilson J. Bioactive materials for periodontal treatment: A comparative study, in biomaterials and clinical applications. Amsterdam: Elsevier; 1987.
 26. Felipe ME, Andrade PF, Novaes AJ, Grisi MF, Souza SL, Taba MJ, et al. Potential of bioactive glass particles of different size ranges to affect bone formation in interproximal periodontal defects in dogs. *J Periodontol*. 2009;**80**(5):808-15. doi: [10.1902/jop.2009.080583](https://doi.org/10.1902/jop.2009.080583). [PubMed: [19405835](https://pubmed.ncbi.nlm.nih.gov/19405835/)].
 27. el-Ghannam A, Ducheyne P, Shapiro IM. Bioactive material template for in vitro synthesis of bone. *J Biomed Mater Res*. 1995;**29**(3):359-70. doi: [10.1002/jbm.820290311](https://doi.org/10.1002/jbm.820290311). [PubMed: [7615587](https://pubmed.ncbi.nlm.nih.gov/7615587/)].
 28. Shapoff CA, Alexander DC, Clark AE. Clinical use of a bioactive glass particulate in the treatment of human osseous defects. *Compend Contin Educ Dent*. 1997;**18**(4):352-4-358 passim. [PubMed: [9452543](https://pubmed.ncbi.nlm.nih.gov/9452543/)].
 29. Nablo BJ, Rothrock AR, Schoenfish MH. Nitric oxide-releasing sol-gels as antibacterial coatings for orthopedic implants. *Biomaterials*. 2005;**26**(8):917-24. doi: [10.1016/j.biomaterials.2004.03.031](https://doi.org/10.1016/j.biomaterials.2004.03.031). [PubMed: [15353203](https://pubmed.ncbi.nlm.nih.gov/15353203/)].
 30. Liu X, Xie Z, Zhang C, Pan H, Rahaman MN, Zhang X, et al. Bioactive borate glass scaffolds: in vitro and in vivo evaluation for use as a drug delivery system in the treatment of bone infection. *J Mater Sci Mater Med*. 2010;**21**(2):575-82. doi: [10.1007/s10856-009-3897-8](https://doi.org/10.1007/s10856-009-3897-8). [PubMed: [19830527](https://pubmed.ncbi.nlm.nih.gov/19830527/)].
 31. Rivallin M, Benmami M, Kanaev A, Gaunand A. Sol-Gel Reactor With Rapid Micromixing. *Chem Eng Res Des*. 2005;**83**(1):67-74. doi: [10.1205/cherd.03073](https://doi.org/10.1205/cherd.03073).
 32. Senthilkumaar S, Porkodi K, Vidyalakshmi R. Photodegradation of a textile dye catalyzed by sol-gel derived nanocrystalline tio2 via ultrasonic irradiation. *J Photochem Photobiol*. 2005;**170**(3):225-32. doi: [10.1016/j.jphotochem.2004.07.005](https://doi.org/10.1016/j.jphotochem.2004.07.005).
 33. Meng Z, Han SB, Kim DH, Park CY, Oh WC. Fabrication of hybrid nio/acf/tio2composites and their photocatalytic activity under visible light. *J Korean Ceram Soc*. 2011;**48**(3):211-6. doi: [10.4191/kcers.2011.48.3.211](https://doi.org/10.4191/kcers.2011.48.3.211).
 34. Finney L, Vogt S, Fukai T, Glesne D. Copper and angiogenesis: unravelling a relationship key to cancer progression. *Clin Exp Pharmacol Physiol*. 2009;**36**(1):88-94. doi: [10.1111/j.1440-1681.2008.04969.x](https://doi.org/10.1111/j.1440-1681.2008.04969.x). [PubMed: [18505439](https://pubmed.ncbi.nlm.nih.gov/18505439/)].
 35. Gerard C, Bordeleau LJ, Barralet J, Doillon CJ. The stimulation of angiogenesis and collagen deposition by copper. *Biomaterials*. 2010;**31**(5):824-31. doi: [10.1016/j.biomaterials.2009.10.009](https://doi.org/10.1016/j.biomaterials.2009.10.009). [PubMed: [19854506](https://pubmed.ncbi.nlm.nih.gov/19854506/)].
 36. Akbari B, Tavandashti MP, Zandrahimi M. Particle size characterization of nanoparticles-a practical approach. *Iranian J Mat Sci Eng*. 2011;**8**(2):48-56.
 37. Bohner M, Lemaitre J. Can bioactivity be tested in vitro with SBF solution?. *Biomaterials*. 2009;**30**(12):2175-9. doi: [10.1016/j.biomaterials.2009.01.008](https://doi.org/10.1016/j.biomaterials.2009.01.008). [PubMed: [19176246](https://pubmed.ncbi.nlm.nih.gov/19176246/)].
 38. Gomez-Vega JM, Saiz E, Tomsia AP, Marshall GW, Marshall SJ. Bioactive glass coatings with hydroxyapatite and Bioglass particles on Ti-based implants. 1. Processing. *Biomaterials*. 2000;**21**(2):105-11. [PubMed: [10632392](https://pubmed.ncbi.nlm.nih.gov/10632392/)].
 39. Yamamuro T, Hench L, Wilson J. CRC handbook of bioactive glasses and glass ceramics. Boca Raton: CRC Press; 1990.
 40. Navarro M, Ginebra MP, Planell JA. Cellular response to calcium phosphate glasses with controlled solubility. *J Biomed Mater Res A*. 2003;**67**(3):1009-15. doi: [10.1002/jbm.a.20014](https://doi.org/10.1002/jbm.a.20014). [PubMed: [14613251](https://pubmed.ncbi.nlm.nih.gov/14613251/)].
 41. Oudadesse H, Dietrich E, Gal YL, Pellen P, Bureau B, Mostafa AA, et al. Apatite forming ability and cytocompatibility of pure and Zn-doped bioactive glasses. *Biomed Mater*. 2011;**6**(3):035006. doi: [10.1088/1748-6041/6/3/035006](https://doi.org/10.1088/1748-6041/6/3/035006). [PubMed: [21505231](https://pubmed.ncbi.nlm.nih.gov/21505231/)].
 42. Brink M, Turunen T, Happonen RP, Yli-Urpo A. Compositional dependence of bioactivity of glasses in the system Na2O-K2O-MgO-CaO-B2O3-P2O5-SiO2. *J Biomed Mater Res*. 1997;**37**(1):114-21.
 43. Ling Feng Q, Nam Kim T, Wu J, Seo Park E, Ock Kim J, Young Lim D, et al. Antibacterial effects of ag-hap thin films on alumina substrates. *Thin Solid Films*. 1998;**335**(1-2):214-9. doi: [10.1016/s0040-6090\(98\)00956-0](https://doi.org/10.1016/s0040-6090(98)00956-0).
 44. Chen W, Liu Y, Courtney HS, Bettenga M, Agrawal CM, Bumgardner JD, et al. In vitro anti-bacterial and biological properties of magnetron co-sputtered silver-containing hydroxyapatite coating. *Biomaterials*. 2006;**27**(32):5512-7. doi: [10.1016/j.biomaterials.2006.07.003](https://doi.org/10.1016/j.biomaterials.2006.07.003). [PubMed: [16872671](https://pubmed.ncbi.nlm.nih.gov/16872671/)].
 45. Devadathan D, Raveendran R. Polyindole based nickel-zinc oxide nanocomposite-characterization and antifungal studies. *Int J Chem Eng Appl*. 2014;**5**(3):240.
 46. Hussain SM, Hess KL, Gearhart JM, Geiss KT, Schlager JJ. In vitro toxicity of nanoparticles in BRL 3A rat liver cells. *Toxicol In Vitro*. 2005;**19**(7):975-83. doi: [10.1016/j.tiv.2005.06.034](https://doi.org/10.1016/j.tiv.2005.06.034). [PubMed: [16125895](https://pubmed.ncbi.nlm.nih.gov/16125895/)].
 47. Douli M, Naghsh N, Setorki M. Comparison of the effects of silver nanoparticles on pathogenic bacteria resistant to beta-lactam antibiotics (ESBLs) as a prokaryote model and Wistar rats as a eukaryote model. *Med Sci Monit Basic Res*. 2013;**19**:103-10. doi: [10.12659/MSMBR.883835](https://doi.org/10.12659/MSMBR.883835). [PubMed: [23507904](https://pubmed.ncbi.nlm.nih.gov/23507904/)].
 48. Gibson JD, Khanal BP, Zubarev ER. Paclitaxel-functionalized gold nanoparticles. *J Am Chem Soc*. 2007;**129**(37):11653-61. doi: [10.1021/ja075181k](https://doi.org/10.1021/ja075181k). [PubMed: [17718495](https://pubmed.ncbi.nlm.nih.gov/17718495/)].
 49. El-Kady A, Ali A. Fabrication and characterization of ZnO modified bioactive glass nanoparticles. *Ceramics International*. 2012;**38**(2):1195-204. doi: [10.1016/j.ceramint.2011.07.069](https://doi.org/10.1016/j.ceramint.2011.07.069).
 50. Lin CC, Huang LC, Shen P. Na 2 CaSi 2 O 6-P 2 O 5 based bioactive glasses. Part 1: elasticity and structure. *J Non-Cryst Solids*. 2005;**351**(40):3195-203.
 51. Sakai H, Ito E, Cai RX, Yoshioka T, Kubota Y, Hashimoto K, et al. Intracellular Ca2+ concentration change of T24 cell under irradiation in the presence of TiO2 ultrafine particles. *Biochim Biophys Acta*. 1994;**1201**(2):259-65. [PubMed: [7947940](https://pubmed.ncbi.nlm.nih.gov/7947940/)].
 52. Neel EA, Ahmed I, Pratten J, Nazhat SN, Knowles JC. Characterisation of antibacterial copper releasing degradable phosphate glass fibres. *Biomaterials*. 2005;**26**(15):2247-54. doi: [10.1016/j.biomaterials.2004.07.024](https://doi.org/10.1016/j.biomaterials.2004.07.024). [PubMed: [15585226](https://pubmed.ncbi.nlm.nih.gov/15585226/)].